Seeded High Yield Synthesis of Short Au Nanorods in Aqueous Solution

Tapan K. Sau and Catherine J. Murphy*

Department of Chemistry and Biochemistry, University of South Carolina, 631 Sumter Street, Columbia, South Carolina 29208

Received March 1, 2004. In Final Form: May 11, 2004

Short gold nanorods of average lengths ranging between 20 and 100 nm (with corresponding aspect ratios of 2 and 4) were synthesized in excellent yield (∼97%). These nanorods were characterized by dark-field microscopy, UV−visible spectrophotometry, and transmission electron microscopy. Temporal evolution of rod shape had also been followed by UV−visible spectrophotometry and transmission electron microscopy and indicates that the nanorods briefly increase in length, then increase slightly in width, as they grow. The effect of the synthetic parameters on the rod dimension and yield was explored to find out suitable conditions to produce short nanorods; short nanorods have both plasmon bands in the visible region of the spectrum, which is a valuable property for sensor applications.

Introduction

Synthesis of nanostructures via simple wet-chemical methods is one of the favored routes toward the cost-effective large-scale production of nano-building blocks. However, achieving control over the growth of nanostructures leading to proper dimensional confinement via wet-chemical methods is a challenging task. Of late, there has been substantial progress in controlling the size and shape of nanoparticles by restricted growth obtained by the introduction of templates,[1] surface capping agents,[2] and other physicochemical means.[3] Solution phase preparation of metallic nanorods and nanowires is a challenging task for two reasons. First, surface energy favors the formation of spherical particles. Second, most metals crystallize in highly symmetric cubic lattices. Therefore, soft and rigid templates[1] had been used to achieve rod-shaped metal nanostructures. However, surface capping agents, such as cetyltrimethylammonium bromide (CTAB),[4] benzyldimethylhexadecylammonium chloride,[5] tetraoctylphosphineoxide,[6] oleic acid,[7] and so forth, had been successfully used for the creation of rod-shaped nanoparticles. Short aspect ratio Au nanorods are especially interesting because of their optical properties: they exhibit the transverse as well as intense longitudinal plasmon bands in the visible region of the spectrum, making them promising candidates for sensing and imaging applications.[8] In addition, metallic nanorods that are 100 nm × 200 nm are being explored for gene delivery applications.[9]

We have reported[2c,4a,b,10] the synthesis of gold and silver nanorods/wires with relatively high aspect ratios by aqueous seeded and nonseeded growth methods. The synthesis relies on the reduction of metal salt by a weak reducing agent in the presence of preformed metallic seed particles. On the basis of electron diffraction analysis and high-resolution transmission electron microscopy (TEM), we have proposed[11] a mechanism in which gold nanorods evolve by the symmetry breaking of face-centered cubic metallic structures by preferential adsorption of capping agents to different crystal faces to produce anisotropic penta-twinned particles. Recently, Gai and Harmer[12] and Xia et al.[13] studied similar systems and gathered further evidence supporting this mechanism of rod evolution. To make gold nanorods, we have shown[2c] that the use of silver nitrate in the seeded synthesis method improved the yield as well as subtly changed the shape of gold nanorods. Similar observations were previously made in the electrochemical synthesis of Au rods.[4c] Nikoobakht and El-

* Corresponding author. E-mail: murphy@mail.chem.sc.edu.

(1) (a) Pileni, M. P.; Ninham, B. W.; Gulik-Krzywicki, T.; Tanori, J.; Lisiecki, I.; Filankembo, A. *Adv. Mater.* **1999**, *11*, 1358. (b) Qi, L. M.; Ma, J. M.; Cheng, H. M.; Zhao, Z. G. *J. Phys. Chem. B* **1997**, *101*, 3460. (c) Li, M.; Schnablegger, M. H.; Mann, S. *Nature* **1999**, *402*, 393. (d) Sloan, J.; Wright, D. M.; Woo, H. G.; Bailey, S.; Brown, G.; York, A. P. E.; Coleman, K. S.; Hutchison, J. L.; Green, M. L. H. *Chem. Commun.* **1999**, 699. (e) Kyotani, T.; Tsai, L. F.; Tomita, A. *Chem. Commun.* **1997**, 701. (f) Martin, B. R.; Dermody, D. J.; Reiss, B. D.; Fang, M. M.; Lyon, L. A.; Natan, M. J.; Mallouk, T. E. *Adv. Mater.* **1999**, *11*, 1021. (g) van der Zande, B. M. I.; Bohmer, M. R.; Fokkink, L. G. J.; Schonenberger, C. *Langmuir* **2000**, *16*, 451. (h) Cepak, V. M.; Martin, C. R. *J. Phys. Chem. B* **1998**, *102*, 9985. (i) Thurn-Albrecht, T.; Schotter, J.; Kastle, G. A.; Emley, N.; Shibauchi, T.; Krusin-Elbaum, L.; Guarini, K.; Black, C. T.; Tuominen, M. T.; Russel, T. P. *Science* **2000**, *290*, 2126.

(2) (a) Manna, L.; Milliron, D. J.; Meisel, A.; Scher, E. C.; Alivisatos, A. P. *Nat. Mater.* **2003**, *2*, 382. (b) Sun, Y.; Xia, Y. *Science* **2002**, *298*, 2176. (c) Jana, N. R.; Gearheart, L.; Murphy, C. J. *Adv. Mater.* **2001**, *13*, 1389. (d) Bradley, J. S.; Tesche, B.; Busser, W.; Maase, M.; Reetz, M. T. *J. Am. Chem. Soc.* **2000**, *122*, 4631. (e) Antonietti, M.; Grohn, F.; Hartman, J.; Bronstein, L. *Angew. Chem., Int. Ed. Engl.* **1997**, *36*, 2080. (f) Ahmadi, T. S.; Wang, Z. L.; Green, T. C.; Henglein, A.; El-Sayed, M. A. *Science* **1996**, *272*, 1924.

(3) Jin, R.; Cao, Y. C.; Hao, E.; Metraux, G. S.; Schatz, G. C.; Mirkin, C. A. *Nature* **2003**, *425*, 487.

(4) (a) Murphy, C. J.; Jana, N. R. *Adv. Mater.* **2002**, *14*, 80. (b) Jana, N. R.; Gearheart, L.; Murphy, C. J. *J. Phys. Chem. B* **2001**, *105*, 4065. (c) Ying, Y.; Chang, S. S.; Lee, C. L.; Wang, C. R. C. *J. Phys. Chem. B* **1997**, *101*, 6661.

(5) Nikoobakht, B.; El-Sayed, M. A. *Chem. Mater.* **2003**, *15*, 1957.

(6) (a) Peng, Z. A.; Peng, X. G. *J. Am. Chem. Soc.* **2002**, *124*, 3343. (b) Peng, X. G.; Manna, L.; Yang, W. D.; Wickham, J.; Scher, E.; Kadavanich, A.; Alivisatos, A. P. *Nature* **2000**, *404*, 59.

(7) Puntes, V. F.; Krishnan, K. M.; Alivisatos, A. P. *Science* **2001**, *291*, 2115.

(8) (a) Haynes, C. L.; Van Duyne, R. P. *J Phys. Chem. B* **2001**, *105*, 5599**.** (b) Sun, Y.; Xia, Y. *Analyst* **2003**, *128*, 686. (c) Sönnichsen, C.; Franzl, T.; Wilk, T.; von Plessen, G.; Feldmann, J.; Wilson, O.; Mulvaney, P. *Phys. Rev. Lett.* **2002**, *88*, 077402.

(9) Salem, A. K.; Searson, P. C.; Leong, K. W. *Nat. Mater.* **2003**, *2*, 668.

(10) (a) Caswell, K. K.; Bender, C. M.; Murphy, C. J. *Nano Lett.* **2003**, *3*, 667. (b) Jana, N. R.; Gearheart, L.; Murphy, C. J. *Chem. Commun.* **2001**, 617. (c) Gao, J.; Bender, C. M.; Murphy, C. J. *Langmuir* **2003**, *19*, 9065. (d) Busbee, B. D.; Obare, S. O.; Murphy, C. J. *Adv. Mater.* **2003**, *15*, 414.

(11) Johnson, C. J.; Dujardin, E.; Davis, S. A.; Murphy, C. J.; Mann, S. *J. Mater. Chem.* **2002**, *12*, 1765.

(12) Gai, P. L.; Harmer, M. A. *Nano Lett.* **2002**, *2*, 771.

(13) Sun, Y.; Mayers, B.; Herricks, T.; Xia, Y. *Nano Lett.* **2003**, *3*, 955.

10.1021/la049463z CCC: $27.50
Published on Web 06/19/2004

Table 1. Produced Gold Nanorod Dimensions and Yield, with Corresponding Initial Concentrations of Reactants[a]

product		reaction conditions				
dimension[b] (length × width)	yield[b]	$[Au^{3+}]$, M	$[Ag^{+}]$, M	[AA], M	$[Au]_{seed}$, M	figure number
87 (±17) × 42 (±10)	97 (±3)	4.0×10^{-4}	6.0×10^{-5}	6.4×10^{-4}	1.25×10^{-7}	2a
64 (±12) × 24 (±6)	97 (±3)	4.0×10^{-4}	6.0×10^{-5}	6.4×10^{-4}	2.5×10^{-7}	2b
62 (±10) × 23 (±3)	93 (±5)	4.0×10^{-4}	6.0×10^{-5}	6.4×10^{-4}	5.0×10^{-7}	2c
50 (±5) × 15 (±3)	90 (±5)	4.0×10^{-4}	6.0×10^{-5}	6.4×10^{-4}	1.25×10^{-6}	2d
475 (±24) × 15 (±2)	55 (±12)	4.0×10^{-4}		6.4×10^{-4}	5.0×10^{-7}	2e
80 (±15) × 40 (±10)	97 (±3)	6.0×10^{-4}	6.0×10^{-5}	9.6×10^{-4}	5.0×10^{-7}	6a
54 (±10) × 14 (±3)	90 (±5)	3.0×10^{-4}	6.0×10^{-5}	2.4×10^{-4}	5.0×10^{-7}	6b
22 (±3) × 6 (±2)	88 (±5)	1.0×10^{-4}	6.0×10^{-5}	1.6×10^{-4}	5.0×10^{-7}	6c
90 (±11) × 15 (±2)	57 (±14)	4.0×10^{-4}		3.0×10^{-3}	5.0×10^{-7}	7a
75 (±8) × 10 (±2)	55 (±14)	4.0×10^{-4}		3.0×10^{-3}	1.5×10^{-6}	7b
50 (±6) × 10 (±2)	55 (±17)	4.0×10^{-4}		3.0×10^{-3}	2.5×10^{-6}	7c

[a] Reactants were added in the order indicated, from left to right. All reactions were run in 5 mL of aqueous 9.5×10^{-2} M CTAB solutions at room temperature. [b] A total of 600 particles from three identical batches (200 particles from each) were counted to calculate the rod yield, and 150 nanorods (50 nanorods from each identical batch) were considered to calculate the average rod dimension. Rod yield is given by (number of rods)/(total number of particles) × 100%. The error bars in the dimensions correspond to one standard deviation in each case.

Sayed[5] obtained Au rods of varied aspect ratio in solution by varying the amount of silver nitrate for a given amount of gold. They reported a very high yield of Au nanorods when they used surfactant-stabilized Au seeds. Here, we extended the above methods to produce a very high yield of short Au nanorods of average lengths ranging from 20 to 100 nm in a controllable manner. We carried out a systematic study to observe the influence of various reaction parameters on the rod dimension. We have shown that in addition to the concentration ratio of Au seed to Au^{3+} ions, the reducing agent (L-ascorbic acid, AA) and capping agent played important roles in controlling the aspect ratio as well as the yield of Au nanorods. We also report on the light-scattering properties of both short and long nanorods, as observed by dark-field microscopy.

Experimental Section

Chemicals. $HAuCl_4 \cdot 3H_2O$ (99.9%), $NaBH_4$ (99%), AA (99+%), CTAB (99%), and $AgNO_3$ (99+%) were used as purchased (Aldrich). Ultrapure deionized water (DI; Continental Water Systems) was used for all solution preparations and experiments. Glassware was cleaned by soaking in aqua regia and finally washing with DI water.

Methods. *Preparation of Au Seeds.* In a typical procedure, 0.250 mL of an aqueous 0.01 M solution of $HAuCl_4 \cdot 3H_2O$ was added to 7.5 mL of a 0.10 M CTAB solution in a test tube (glass or plastic). The solutions were gently mixed by the inversion. The solution appeared bright brown-yellow in color. Then, 0.600 mL of an aqueous 0.01 M ice-cold $NaBH_4$ solution was added all at once, followed by rapid inversion mixing for 2 min. Care should be taken to allow the escape of the evolved gas during mixing. The solution developed a pale brown-yellow color. Then the test tube was kept in a water bath maintained at 25 °C for future use. This seed solution was used 2 h after its preparation and could be used over a period of 1 week. This preparation differs from other seed preparations we have used, in that the CTAB surfactant is present at this stage. We prepared gold seeds at four different CTAB concentrations, namely, 9.5×10^{-2}, 7.5×10^{-2}, 5.0×10^{-2}, and 8.0×10^{-3} M. Seeds prepared at 8.0×10^{-3} M CTAB produced non-rod-shaped and phi-shaped rod particles.

Preparation of Au Nanorods. Appropriate quantities of CTAB solution, water, $HAuCl_4$, $AgNO_3$, AA, and seed solutions were taken one by one in the order given (see Table 1) in a test tube and mixed gently by inversion. When the seed solution was added before AA, the reaction became very slow. Therefore, the seed solution was always added after the addition of AA. For example, in a typical experiment, 4.75 mL of 0.10 M CTAB, 0.200 mL of 0.01 M $HAuCl_4 \cdot 3H_2O$, and 0.030 mL of 0.01 M $AgNO_3$ solutions were added in that order, one by one, to a test tube, followed by gentle mixing by inversion. The solution at this stage appeared bright brown-yellow in color. Then 0.032 mL of 0.10 M AA was added to it. The solution became colorless upon addition and mixing of AA. Finally, 0.010 mL of seed solution was added, and the reaction mixture was gently mixed for 10 s and left undisturbed for at least 3 h.

Characterization. Absorption spectra of the solutions were taken on a CARY 500 Scan UV−vis−NIR spectrophotometer. Dark-field microscopy images were taken in a Nikon dark-field microscope system with an oil immersion objective. TEM images were obtained either with a Hitachi H-8000 or a JEOL JEM-100CX II electron microscope. The TEM grids were prepared as follows: Typically 1.5 mL of the solution was centrifuged for 12 min at a speed of 14 000 rpm to precipitate the solid. The colorless supernatant was discarded. The solid residue was redispersed in 1.5 mL of DI water and centrifuged again. Finally the solid residue was dispersed in a suitable volume of DI water depending on the quantity of the residue. A total of 7 μL of this solution was dropcast on the TEM grid and allowed to dry in the open atmosphere. Elemental analysis was carried out on a Hitachi 2500 Delta scanning electron microscope by X-ray energy dispersive analysis (EDAX).

Results and Discussion

Short gold nanorods are of interest for optical sensing applications because both plasmon bands are in the visible region of the spectrum. Our previous syntheses of short gold nanorods (aspect ratio less than 6) produced large amounts of spherical side products that can be difficult to separate. The present study was undertaken to find the appropriate reaction conditions to prepare short gold nanorods, in high yield, by room-temperature colloid chemical methods.

The procedure we have used here for making gold nanorods has the same ingredients as others;[2c,4b,5,10d] however, we demonstrate here how the rod length and width change with time and with variations in concentrations of the reducing agent and stabilizing surfactant, in addition to [seed]/$[Au^{3+}]$ ratio. Depending on the reaction conditions, the rod formation continues for 1 h or so as judged spectrophotometrically (Figure 1). The longitudinal plasmon band begins to appear in 1 or 2 min, and interestingly, it blue-shifts as the rods develop with time. The nanorods at various stages of their growth process were also characterized by TEM to obtain a vivid picture of their evolution (Supporting Information Figure 1). The trend in the change in longitudinal plasmon peak position with time seems to be in agreement with the change in aspect ratio (as opposed to length alone) of the developing rods (Figure 1); the aspect ratio of the rods increases quickly, then slowly decreases over time. Schatz et al. have described a theoretical framework that correlates

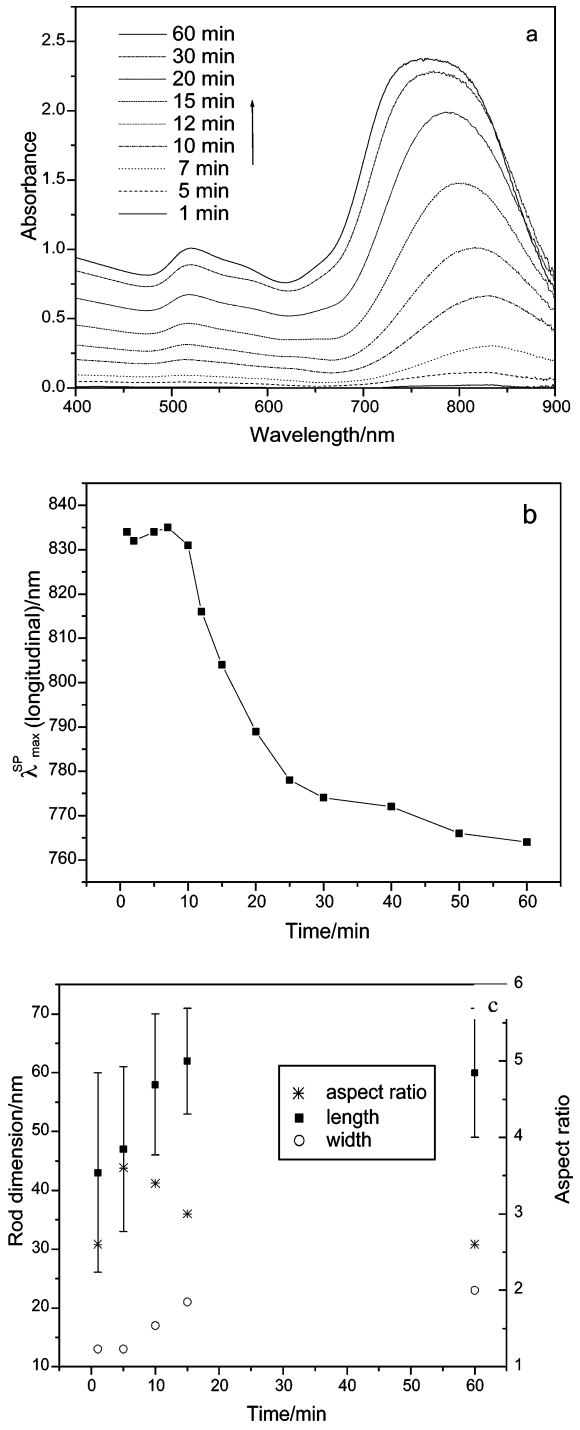

Figure 1. (a) Visible−NIR absorption spectra of a representative gold nanorod solution growing from gold seeds as a function of time from 1 to 60 min after addition of seed to the growth solution. (b) Variation of longitudinal plasmon band maximum with time. Conditions: $[CTAB] = 9.5 \times 10^{-2}$ M, $[HAuCl_4] = 4.0 \times 10^{-4}$ M, $[AgNO_3] = 6.0 \times 10^{-5}$ M, $[AA] = 6.4 \times 10^{-4}$ M, and $[Au]_{seed} = 5.0 \times 10^{-7}$ M. (c) Temporal evolution of nanorod length, width, and aspect ratio based on TEM micrographs (Supporting Information).

plasmon band position with nanoparticle shape, in terms of aspect ratio, that coincides with our data.[14]

Silver nitrate was essential for the preparation of short Au nanorods in very high yield. For example, when silver nitrate was not added, longer rods with a large fraction of non-rod-shaped particles were produced (Figure 2; compare part c with part e, and Table 1, compare the third row with the fifth). The role of silver nitrate is not clearly understood at this moment. We proposed[2c] that $AgNO_3$ forms AgBr in the presence of CTAB and AgBr adsorbs differentially to the facets of Au particles, thereby restricting their growth to the rod shape. Nikoobakht and El-Sayed support the notion of AgBr on the Au rod surface and proposed that AgBr decreases the charge density and, hence, repulsion between the neighboring headgroups resulting in CTAB template elongation; CTAB in this interpretation is thought to function as a soft template (it makes the aspect ratio ∼4 micelles in water).[5] In our experiments, the final nanorod samples contained at most ∼4% silver, according to EDAX; but this measurement does not distinguish between silver that is alloyed within gold nanorods and that merely adsorbed to the surface in either elemental or compound form.

It is believed that well-organized CTAB molecules not only help to maintain one-dimensional growth but also dictate the approach rate of gold ions and AA to the seed particles. There is evidence that CTAB forms bilayers on gold nanorods and that these bilayers may help "zip" along the long axis of the nanorods to promote a rodlike shape.[10c,15] In fact, the kinetics of reduction of gold ions to atomic gold (as followed by the increase in absorbance at 440 nm)[16] showed that the reduction was slower in the presence of silver nitrate (Figure 3). Furthermore, we observed that a decrease or an increase in the amount of silver nitrate added could lead to the formation of non-rod-shaped (quasi spherical or irregularly grown spiked) particles. Therefore, the proper kinetics of the growth step too played a role in the formation of rods in high yield, as was observed by Peng et al. in the case of CdSe nanocrystals.[6,17]

In the case of gold nanorods made without silver ion as an additive, the nanorods are obtained in relatively low yield (many spheres are present) but are quite long, with aspect ratios of ∼20. In this method, in the presence of silver ion, the gold nanorod yield is nearly quantitative, but the highest aspect ratio obtainable is ∼5. Understanding the mechanism at this point is complicated by the preliminary result that these short rods, made with silver ion, appear to have a different crystallography than the ones made without silver ion.[11] In our previous work without silver ion, the gold nanorods were penta-tetrahedral twins, in which five {111} triangular facets were on the ends of the rods, and {100} facets were on the long sides of the rods.[11] In the present case, according to very preliminary high-resolution TEM images, these short gold nanorods made in the presence of silver ions are single crystalline, with possibly {111} facets on the long side of the rods. Silver bromide is the likely form of silver during the synthesis (as a result of the ∼0.1 M bromide present in the seed stage from CTAB; and silver bromide is not reduced to silver metal by ascorbate). Silver bromide can also form thin films epitaxially on Au{111} that can undergo reconstruction.[18] Also, bromide ions make incommensurate adlayers on both Au{111} and Au{100} that reconstruct depending on surface coverage.[19] Taken together, should our preliminary crystallography result stand, we speculate that bromide adsorbs to the gold seeds; the presence of silver might form silver bromide at the

(14) Kelly, K. L.; Coronado, E.; Zhao, L. L.; Schatz, G. C. *J. Phys. Chem. B* **2003**, *107*, 668.
(15) Nikoobakht, B.; El-Sayed, M. A. *Langmuir* **2001**, *17*, 6368.
(16) Rao, P.; Doremus, R. *J. Non-Cryst. Solids* **1996**, *203*, 202.
(17) Peng, X. G. *Adv. Mater.* **2003**, *15*, 459.
(18) Mason, M. G.; Hansen, J. C. *J. Vac. Sci. Technol., A* **1994**, *12*, 2023.
(19) Magnussen, O. M. *Chem. Rev.* **2002**, *102*, 679.

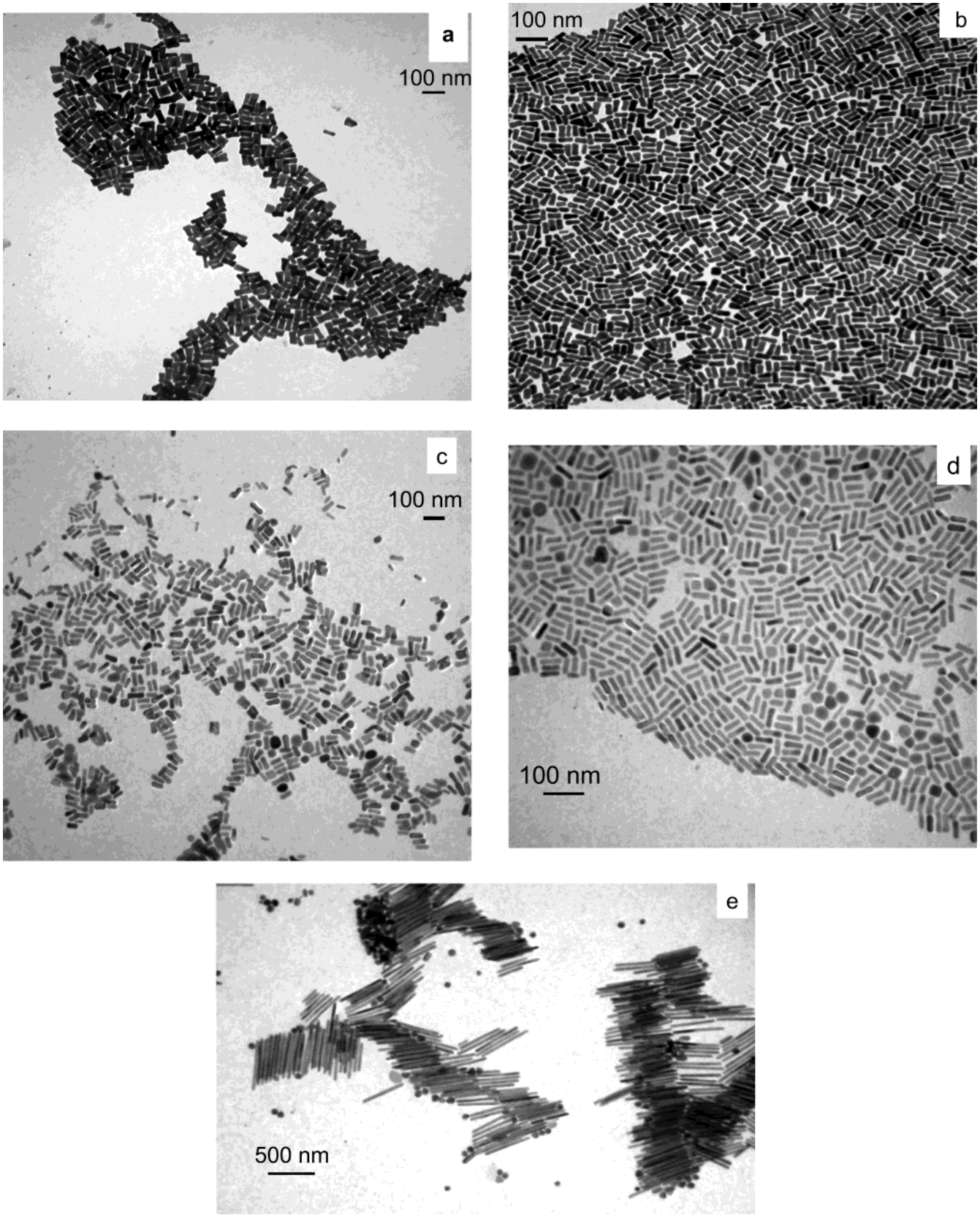

Figure 2. Transmission electron micrographs of dense ensembles of gold nanorods synthesized with different reaction conditions, as a function of seed concentration. $[Au]_{seed}$ were (a) 1.25×10^{-7} M, (b) 2.5×10^{-7} M, (c) 5.0×10^{-7} M, and (d) 1.25×10^{-6} M. The Au seed concentration in part e was the same as in part c. In all cases, $[CTAB] = 9.5 \times 10^{-2}$ M, $[HAuCl_4] = 4.0 \times 10^{-4}$ M, $[AgNO_3] = 6.0 \times 10^{-5}$ M, and $[AA] = 6.4 \times 10^{-4}$ M, except no silver nitrate was used in part e.

gold surface and slow the subsequent gold growth step (which we do observe compared to the situation in the absence of silver); and the slower kinetics results in single crystalline growth of the gold nanorods and the rod morphology results from a silver bromide layer on the {111} faces of the gold nanocrystal, leading to gold reduction on other faces to produce a rod with {111} facets on its long sides.

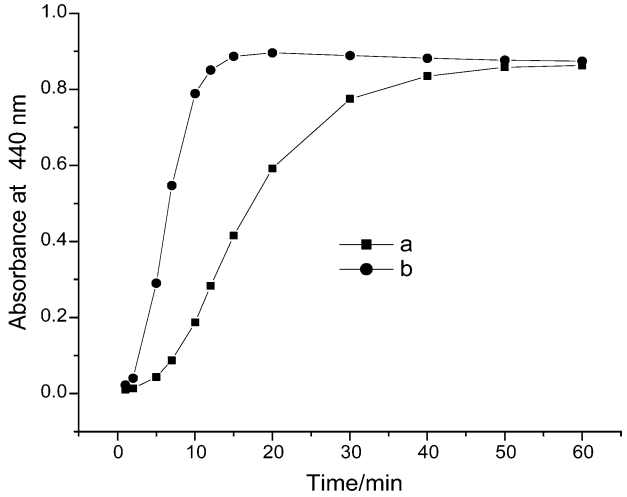

Figure 3. Comparison of rates of formation of atomic gold, as followed by the increase in absorbance at 440 nm in the presence (a) and absence (b) of silver nitrate. Conditions: in all cases, [CTAB] = 9.5×10^{-2} M, [$HAuCl_4$] = 4.0×10^{-4} M, [AA] = 6.4×10^{-4} M, and $[Au]_{seed} = 5.0 \times 10^{-7}$ M. [$AgNO_3$] = 6.0×10^{-5} M in curve a, and no $AgNO_3$ was used in curve b.

Short gold nanorods possess physicochemical properties that are distinctly different from the longer ones. For example, to see the difference in the optical properties between short Au nanorods and long ones, we compared the true color of Rayleigh scattered white light from these samples obtained under dark-field conditions in an optical microscope (Figure 4). As expected, the longer rods preferentially scatter lower-energy orange/red light whereas shorter rods scatter blue-green and yellow light. Also, because both plasmon bands are in the visible for the short rods but only the transverse one is in the visible for the long rods, the short rods scatter more visible light and appear brighter than the long rods (Figure 4). This phenomenon can be exploited for optical sensing and imaging, and studies in this regard, an "optical biochip", are in progress. Other workers have used dark-field microscopy to image metallic nanoparticles of various shapes and have observed that shifts in the color of the scattered light are correlated with the adsorbate's refractive index; this color change can be used for sensing.[20]

For the remainder of the paper, we discuss the influence of the reaction parameters one by one for the synthesis of short gold nanorods.

Effect of Seed Concentration. The rod length decreased, and ultimately very short rods with a small number of spheres appeared, with an increase in the seed concentration, for a given concentration of gold(III) ion. This trend was expected because a lesser quantity of Au^{3+} ions per seed particle was available for the growth.[4a,b,10] The transmission electron micrographs in Figure 2 show the effects of the gold seed concentration and silver nitrate on the rod dimension and yield. As observed previously, the use of a small quantity of silver nitrate had a profound effect on the rod yield (compared to spheres) and in controlling rod dimension. Selection of a proper ratio of seed to gold ion concentrations and addition of an appropriate quantity of $AgNO_3$ resulted in a very high yield (~97%) of rod-shaped particles. Visible−NIR absorption spectra (Figure 5) too showed that the rod yield in the absence of $AgNO_3$ was considerably smaller as judged by the relative values of the longitudinal plasmon absorbance. Figure 5 shows that in the presence of $AgNO_3$ there was a red shift of the longitudinal plasmon absorbance peak position upon an increase in seed concentration. Furthermore, in addition to the usual transverse and longitudinal plasmon absorbance peaks, one additional medium energy peak could be observed in the absorption spectra; depending on the faceting of the ends of the rods, additional plasmon bands can be observed.[14] The red shift with the decrease in rod length appeared to be contradictory but was consistent with their increasing aspect ratio, as a result of the simultaneous decrease in rod width (Table 1).[14]

Effect of Au^{3+} Ion Concentration. It had been noted in the previous section that the rod dimension strongly depends on the total amount of gold ions present in the solution. The variation in rod dimension and yield due to the variation in Au^{3+} ion concentration was again observed to be sensitively dependent on both $[Au]_{seed}$ and [CTAB]. For example, for a $[Au]_{seed} = 5 \times 10^{-7}$ M and [CTAB] = 9.5×10^{-2} M, we varied the Au^{3+} ion concentration between 1.0×10^{-4} and 8.0×10^{-4} M, keeping always [AA] = 1.6-[Au^{3+}], and observed that well-defined rod shapes could be obtained up to [Au^{3+}] ~ 6.0×10^{-4} M. The representative TEM images given in Figure 6 demonstrate the effect of [Au^{3+}] variation on the rod dimension. The ends of the rods appeared more rounded with the decrease in [Au^{3+}]. Visible−NIR absorption spectra of the samples showed that in this case too the shift in the lowest energy plasmon absorption peak position was in agreement with the variation in the aspect ratio of the rods.

Effect of AA Concentration. The rod length can also be varied by variation in the AA concentration. The rod length decreases with an increase in [AA] keeping all other conditions the same. Thus, by increasing the [AA] and manipulating the $[Au]_{seed}/[Au^{3+}]$ ratio one can form short Au nanorods in good yield. Figure 7 shows transmission electron micrographs of some short gold nanorod samples prepared with a large excess of AA. Depending on the other factors, the rod length could decrease by one-half to

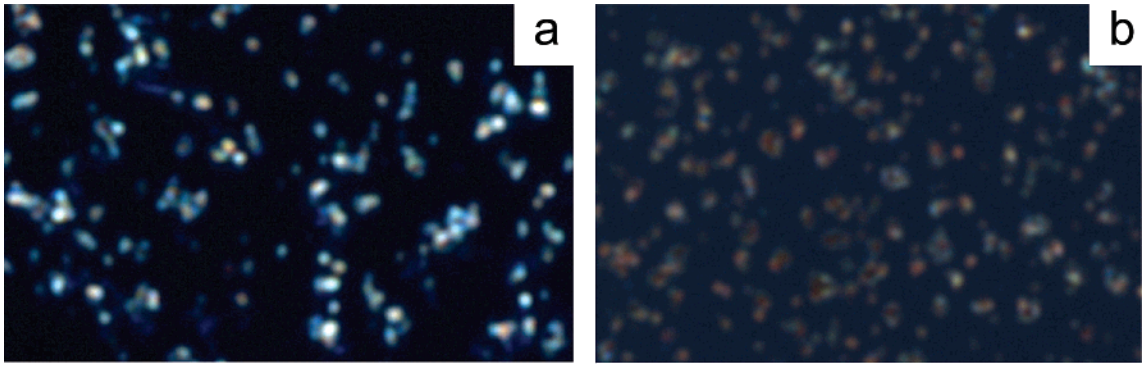

Figure 4. True color images of samples of (a) shorter and (b) longer gold nanorods. The magnification is 100×. The rod dimensions are length/nanometer × width/nanometer = 57 (±11) × 19 (±3) and 475 (±24) × 15 (±2) for shorter and longer rods, respectively.

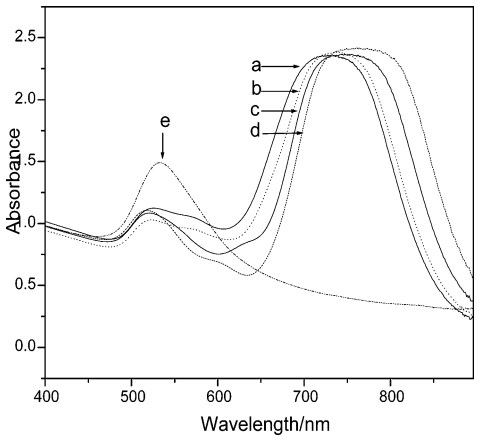

Figure 5. Visible−NIR absorption spectra of gold nanorod samples prepared under various reaction conditions, as a function of Au seed concentration. Conditions are as given in Figure 2, spectra a−e corresponding to samples a−e.

one-fifth for an increase in [AA] from 1.6 to 7.5 times the $[Au^{3+}]$ (i.e., an increase from small excess to 5 times the stoichiometric amount of AA required for the reduction of Au^{3+} ions to Au^0). A comparison of the TEM image in Figure 7a with that in Figure 1e corroborates this fact. Peng et al. observed in the case of the CdSe system[6,15] that there was a greater tendency to form spherical particles under the condition of faster supply of monomer growth units to the seeds. The decrease in rod yield in our present case also seemed to be due to the very fast formation and supply of growth units (Au^0) to the seeds in the presence of a large excess of reducing agent (AA), thereby inducing the growth of seed particles in all directions and forming more spherical particles. It is not clear why hardly any rods were obtained under such a large excess of AA, when silver nitrate was added to the system. Perhaps silver ions were reduced to atomic silver (although others have argued against this)[5] and, hence, were not available for the participation in template elongation via the decrease in headgroup charge of CTAB molecules by forming AgBr.

Effect of CTAB Concentration. Rod length decreases, whereas the width of the rods increases slightly, upon decreasing CTAB concentration in the absence of $AgNO_3$.

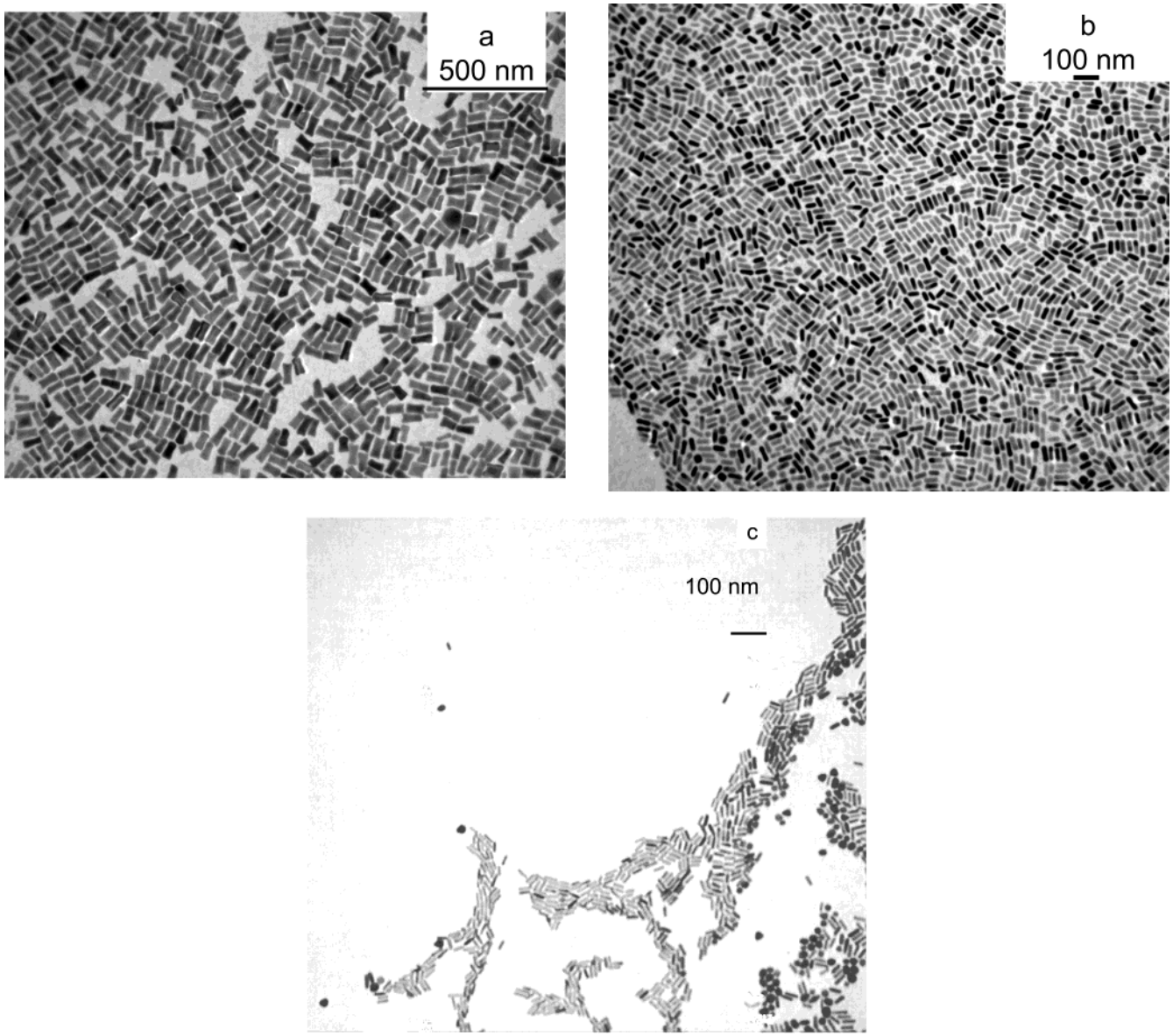

Figure 6. Transmission electron micrographs of gold nanorods synthesized with different amounts of gold salt for a constant seed concentration. In all cases, [CTAB] = 9.5×10^{-2} M, $[AgNO_3] = 6.0 \times 10^{-5}$ M, [AA] = 1.6[$HAuCl_4$], and $[Au]_{seed} = 5.0 \times 10^{-7}$ M. [$HAuCl_4$] were 6.0×10^{-4} M in part a, 3.0×10^{-4} M in part b, and 1.0×10^{-4} M in part c.

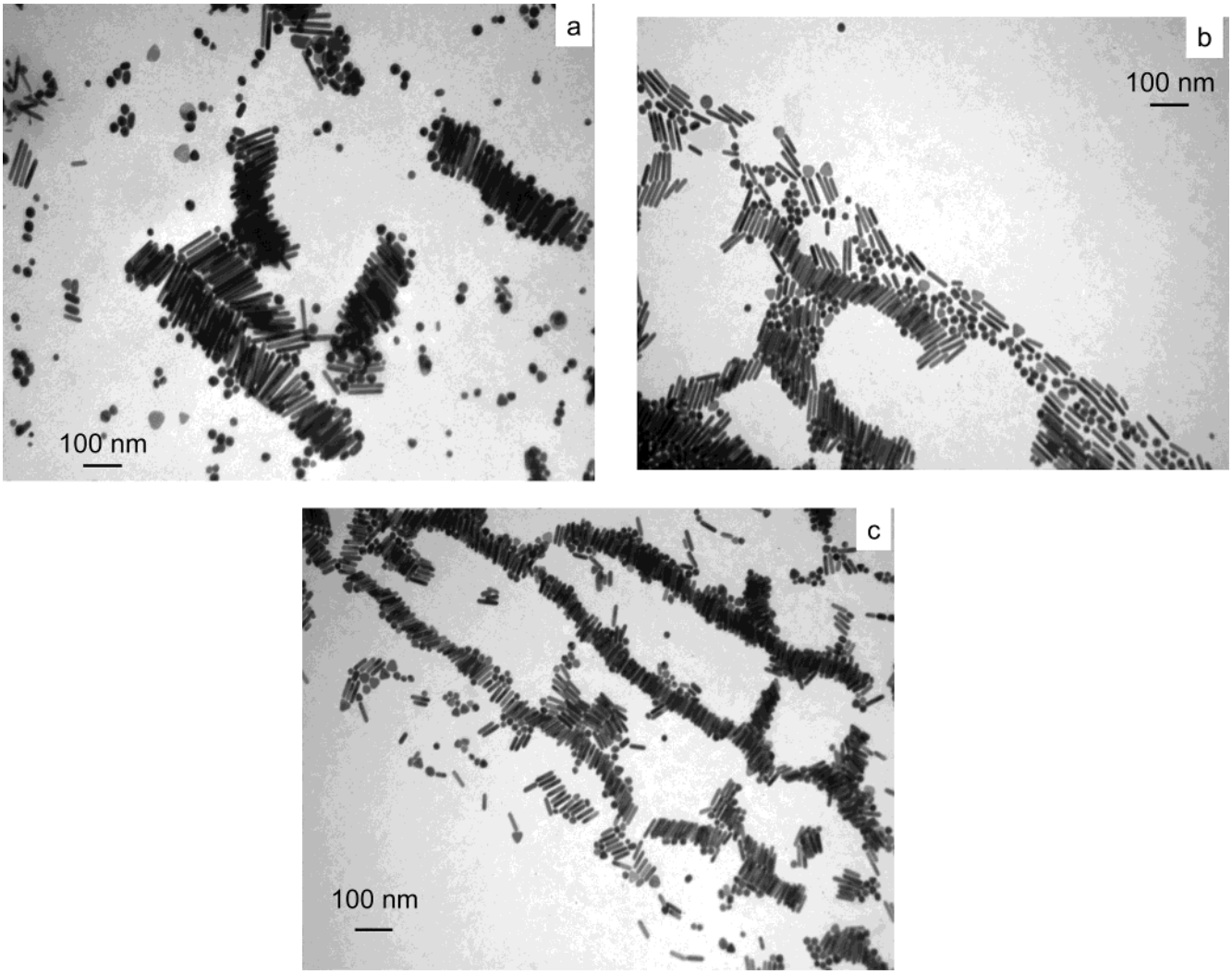

Figure 7. Transmission electron micrographs of short gold nanorods prepared in the absence of silver nitrate. In all cases, [CTAB] = 9.5×10^{-2} M, [$HAuCl_4$] = 4.0×10^{-4} M, and [AA] = 3.0×10^{-3} M. $[Au]_{seed}$ = 5.0×10^{-7} M in part a, 1.5×10^{-6} M in part b, and 2.5×10^{-6} M in part c.

Unfortunately, the yield of rods drops significantly upon decreasing CTAB concentration and, thus, this route becomes unfavorable for the synthesis of short rods in good yield.[21] Furthermore, lower CTAB concentrations can lead to non-rod-shaped particles in the presence of $AgNO_3$ or at higher AA concentrations.

Conclusion

In conclusion, we have systematically varied the synthetic parameters involved in the Au rod formation event and demonstrated how short Au nanorods ranging in length from 20 to 100 nm (aspect ratio from 2 to 4) could be obtained in high yield. Temporal evolution of gold nanorods had been followed spectrophotometrically as well as by TEM, which revealed how the length and width of the developing rods changed with time. Interestingly, the nanorods appear to get longer briefly, then "fill out" and get wider, during the course of the reaction. For the maximum yield of short gold nanorods, silver ion is critical, as is the appropriate concentrations of all other reagents. In the absence of silver ion, longer gold nanorods can be obtained, but significant amounts of spherical side products are produced.

Supporting Information Available: Transmission electron micrographs of gold nanorods at various stages of their growth. This material is available free of charge via the Internet at http://pubs.acs.org.

LA049463Z

(20) (a) Mock, J. J.; Smith, D. R.; Schultz, S. *Nano Lett.* **2003**, *3*, 485. (b) Raschke, G.; Kowarik, S.; Franzl, T.; Sonnichsen, C.; Klar, T. A.; Feldmann, J.; Nichtl, A.; Kurzinger, K. *Nano Lett.* **2003**, *3*, 935. (c) McFarland, A. D.; Van Duyne, R. P. *Nano Lett.* **2003**, *3*, 1057.

(21) Sau, T. K.; Murphy, C. J. *Mater. Res. Soc. Symp. Proc.* **2004**, *789*, 203−212.